PHYSICAL REVIEW B VOLUME 23, NUMBER 2 15 JANUARY 1981

Excitons in cuprous oxide under uniaxial stress

H.-R. Trebin,* H. Z. Cummins, and J. L. Birman
Department of Physics, The City College of the City University of New York, New York, New York 10031
(Received 10 March 1980)

The energy levels for excitons in Cu_2O under uniaxial stress have been calculated under the assumption of strong mixing between the yellow and green exciton series. The reversal of the order for the strain-split levels of the 2*S* yellow exciton with respect to the 1*S* yellow exciton is explained by two different and competing splitting mechanisms. The results agree well with resonance-enhancement measurements of Waters *et al*. The level assignment as proposed by Agekyan and Stepanov and Fröhlich *et al*. is confirmed.

I. INTRODUCTION

The excitons in Cu_2O have attracted much interest due to some special features of this compound's band structure. Because conduction- and valence-band states are of the same parity, the *S* excitons are accessible only by quadrupole and two-photon transitions in the absence of external fields. Compared to the case of Ge, the spin-orbit split Γ_7^+ and Γ_8^+ valence bands are reversed in their order. Their energy difference is so small that the exciton series, to which they contribute, are strongly mixed. Whereas the dipole active *P* states of the yellow series follow the $1/n^2$ Rydberg law, the level assignment of the *S* and *D* states has been controversial. A very weak line at 17 247 cm^{-1} was accepted as a "2*S*" exciton and a strong line at 17 381 cm^{-1} as a "3*S*" exciton. The *D* states and their splittings were investigated by the Strasbourg group.[2] Speculations arose about the physical origin of the strange level spacings of *S* and *D* states,[2,3] the extremely small oscillator strength of the "2*S*" exciton,[4] and the large oscillator strength of the yellow "3*S*" and *D* excitons.[5] In 1975 Agekyan and Stepanov[6] studied the exciton levels in absorption under an electric and strain field. Owing to the unexpectedly small strain splitting of the "2*S*" exciton, they assumed this state to be the 1*S* level of the green exciton series, without presenting, however, a quantitative analysis to justify their conjecture. The displacement of the reassigned *nS* levels, $n \geq 2$, to energies above the *nP* levels, was attributed to the exchange splitting of ortho- and paraexcitons. Recently Waters *et al.*[7] investigated the yellow series by resonance-enhanced Raman scattering in uniaxially compressed crystals. By tuning the laser through the exciton energies, the states were excited by the quadrupole interaction. The Raman shift was caused by a 109-cm^{-1} phonon of Γ_3^- symmetry. The position of the exciton line was determined at maximum resonance. The symmetry of the excitons could be established by polarization analysis of incident and backscattered light. But the results increased the confusion about the level assignments, since no regularity could be found in the splitting patterns of successive levels. The "3*S*" yellow exciton at 17 381 cm^{-1} showed an extremely large strain splitting and a reversal of the order of the split levels as compared to the yellow 1*S* exciton. The *D* states did not split and were of large oscillator strength. The "2*S*" exciton at 17 247 cm^{-1} was not seen. A conventional perturbative approach to the diagonalization of the effective-mass Hamiltonian, neglecting the mixing of different exciton series, could not explain the data.

Considerable progress towards a solution of the puzzle was made by observations and proposals of Fröhlich *et al.*[8] In two-photon absorption the group detected the weak "2*S*" line at 17 247 cm^{-1} in the unperturbed crystal. Following Agekyan and Stepanov[6] they assigned this line to the 1*S* green exciton. The unusual level spacing was explained by the strong exchange interaction between the 1*S* green and the 2*S* yellow exciton which had been previously labeled "3*S*". The energies were calculated by diagonalization of the effective-mass Hamiltonian for the manifold of the Γ_6^+ conduction-band and Γ_7^+ and Γ_8^+ valence-band states in its spherical form.[9,10] Based upon this information we have reinterpreted the data of Waters *et al.* In Sec. II we describe the model Hamiltonian and some technical details used to solve the eigenvalue problem. A connection between the present methods of solution and the perturbation theory applied previously[7] is made. In Sec. III the numerical solution is presented and compared with the measurements of Waters *et al.*[7] The results and the material constants determined are discussed. Predictions are made for the exciton energies under stress parallel to the [111] direction, for which no experimental data exist.

 © 1981 The American Physical Society

II. MODEL HAMILTONIAN AND EIGENVALUE PROBLEM

A. Invariant expansion

According to the discussion of Fröhlich *et al.*[8] it is necessary to treat carefully the coupling between the yellow and the green exciton series. Therefore in the hole kinetic energy T_h of the effective-mass Hamiltonian the entire manifold of the spin-orbit split Γ_5^+ valence-band states has to be taken into account. T_h and the corresponding strain Hamiltonian are presented, for instance, in Ref. 11 as a polynomial in the components k_l of the hole momentum vector, in the $I=1$ angular momentum matrices I_l, and the Pauli matrices σ_l^h, $l=1,2,3$. For the following symmetry analysis of the excitonic states an important remark has to be made concerning this expansion. The valence-band states transform according to the representation $\Gamma_5^+\times\Gamma_6^+=\Gamma_7^+ +\Gamma_8^+$ of the point group O_h, where Γ_6^+ is the representation for the internal spin. Since $\Gamma_5^+=\Gamma_2^+\times\Gamma_4^+$, and since Γ_4^+ and Γ_6^+ result from a reduction of the irreducible representations D_1^+ and $D_{1/2}^+$ of the orthogonal group $O(3)$, we can use the representation matrices.

$$\begin{aligned}&\Gamma_2^+(g)\times D_1^+(g)\quad\text{for } \Gamma_5^+,\\ &D_{1/2}^+(g)\quad\text{for } \Gamma_6^+,\end{aligned}\tag{1}$$

where $g\epsilon O_h$.[12] $T_h(\vec{k})$ is a 6×6 perturbation matrix in a basis of the zone-center valence-band states and must be invariant under any cubic symmetry operation acting on these states and the $\vec{k}$ vector. This implies the relation

$$\begin{aligned}&[\Gamma_2^+(g)\times D_1^+(g)\times D_{1/2}^+(g)]T_h(g^{-1}\vec{k})\\ &\quad\times[\Gamma_2^+(g^{-1})\times D_1^+(g^{-1})\times D_{1/2}^+(g^{-1})]\\ &\qquad=[D_1^+(g)\times D_{1/2}^+(g)]T_h(g^{-1}\vec{k})[D_1^+(g^{-1})\times D_{1/2}^+(g^{-1})]\\ &\qquad=T_h(\vec{k}).\end{aligned}\tag{2}$$

$\Gamma_2^+(g)$ cancels $\Gamma_2^+(g^{-1})=\Gamma_2^+(g)^{-1}$, since it is a c number. Thus the invariant expansion of T_h is identical to that for a valence-state manifold transforming according to $D_1^+(g)\times D_{1/2}^+(g)=\Gamma_4^+(g)\times\Gamma_6^+(g)$, $g\epsilon O_h$. Whenever an eigenstate is analyzed for its symmetry in this pseudospin formalism it must be remembered that the basis functions transform like an $(I=1)\times(S_h=\frac{1}{2})$ angular momentum state multiplied by a function of Γ_2^+ symmetry.[12,13]

The current data on band parameters for Cu_2O are rather uncertain. Hence we restrict ourselves to the most important terms of the effective-mass Hamiltonian which adequately describe the features of the excitonic spectra. Apart from the $\vec{k}$-independent spin-orbit interaction and the exchange interaction all spin-independent terms are omitted; for the hole kinetic energy only the spherical terms are retained. For the relative electron-hole motion, then, the following Hamiltonian remains:

$$\begin{aligned}&H_x=H_0+H_{\text{ex}}+H_d,\\ &H_0=\tfrac{1}{3}\lambda(\vec{I}\cdot\vec{\sigma}^h)+\frac{1}{\hbar^2}[p^2-3\mu(p^{(2)}I^{(2)})]-\frac{2}{r}-q\delta(\vec{r}),\\ &H_{\text{ex}}=\tfrac{1}{2}c(1-\vec{\sigma}^e\cdot\vec{\sigma}^h)\delta(\vec{r}),\\ &H_d=x_h+\begin{cases}-\sqrt{6}\,x_uI_0^{(2)} & \text{for stress }\|[100]\\ -\sqrt{6}\,x_u'I_0^{(2)} & \text{for stress }\|[111]\\ -\sqrt{6}\,x_rI_0^{(2)}-x_{na}(I_2^{(2)}+I_{-2}^{(2)}) & \\ \qquad\text{for stress }\|[110].\end{cases}\end{aligned}\tag{3}$$

Atomic units are used, i.e., the energy is measured in effective Rydbergs,

$$R=\frac{m_re^4}{2\hbar^2\epsilon_0^2},$$

and the length in effective Bohr radii:

$$a=\frac{\epsilon_0\hbar^2}{m_re^2}.$$

Here $m_r^{-1}=m_e^{-1}+\gamma_1^h/m$, m_e denoting the conduction-band mass, m the free-electron mass, and γ_1^h the mean inverse valence-band mass.[9] $\lambda=\Lambda/R$ is the spin-orbit splitting, $\mu=(\gamma_1^hm_r/m)\mu_h$ the reduced valence-band splitting parameter μ_h. For the definition of the second-rank spherical tensors $p^{(2)}$ and $I^{(2)}$ see Ref. 14. The central cell correction is simulated by a contact potential of weight $q>O$. The analytic exchange interaction is an invariant expansion[15] of the form derived by Denisov and Makarov,[16] where $c=C/Ra^3$ and

$$C=4\pi e^2\sum_{\vec{K}\neq\vec{0}}\frac{|\langle\Gamma_1^+|e^{i\vec{K}\cdot\vec{r}}|\Gamma_5^+\rangle|}{K^2}\tag{4}$$

is an interband matrix element between the S-type Γ_1^+ conduction-band state and one of the D-type Γ_5^+ valence-band states, $\vec{K}$ denoting a reciprocal-lattice vector. In the strain Hamiltonian H_d the dimensionless strain constants are defined as

$$\begin{aligned}&x_h=(s_{11}+2s_{12})(C_1-D_1)T/R,\\ &x_u=\tfrac{2}{3}(s_{11}-s_{12})D_uT/R,\\ &x_u'=\tfrac{1}{3}s_{44}D_u'T/R,\\ &x_r=\tfrac{1}{4}(x_u+3x_u'),\\ &x_{na}=\tfrac{3}{4}(x_u-x_u').\end{aligned}\tag{5}$$

T is the external stress (negative, if compressive), $D_u=\frac{1}{2}D_2$, $D_u'=\frac{1}{2}D_3$, and C_1-D_1 are deformation potentials for shear and hydrostatic strain[11]; s_{11}, s_{12}, s_{44} denote the cubic elastic compliance constants.

B. Method of solution

1. Hamiltonian without strain

H_0 and H_{ex} are invariant under rotations. Therefore for H_0 the components of angular momentum $\vec{F}=\vec{L}+\vec{J}$ are constants of the motion, where $\vec{L}=\vec{r}\times\vec{p}$, and $\vec{J}=\vec{I}+\frac{1}{2}\vec{\sigma}^h$. H_0+H_{ex} commutes with the components of $\vec{G}=\vec{F}+\frac{1}{2}\vec{\sigma}^e$. Hence we expand the exciton wave function Ψ_x as

$$\Psi_x=\sum f_{LJFGG_z}(r)\,|LJFGG_z\rangle. \tag{6}$$

The kets denote eigenfunctions of G^2, G_z, coupled from eigenstates of L^2, I^2, $(\sigma^h)^2$, $(\sigma^e)^2$ in the following way:

$$|LJFGG_z\rangle \equiv |((L,(I,\sigma^h)J)F,\sigma^e)G,G_z\rangle. \tag{7}$$

H_x, being of even parity, only connects states of $\Delta L=0,\pm2,\pm4,\ldots$. For the even-parity excitonic states the following kets contribute to Ψ_x:

$G=0,\ F=\frac{1}{2}$:

$$|0\tfrac{1}{2}\tfrac{1}{2}00\rangle,\quad |2\tfrac{3}{2}\tfrac{1}{2}00\rangle;$$

$G=1,\ F=\frac{1}{2}$:

$$|0\tfrac{1}{2}\tfrac{1}{2}1G_z\rangle,\quad |2\tfrac{3}{2}\tfrac{1}{2}1G_z\rangle;$$

$G=1,\ F=\frac{3}{2}$:

$$|0\tfrac{3}{2}\tfrac{3}{2}1G_z\rangle,\quad |2\tfrac{3}{2}\tfrac{3}{2}1G_z\rangle,\quad |2\tfrac{1}{2}\tfrac{3}{2}1G_z\rangle; \tag{8}$$

$G=2,\ F=\frac{3}{2}$:

$$|0\tfrac{3}{2}\tfrac{3}{2}2G_z\rangle,\quad |2\tfrac{3}{2}\tfrac{3}{2}2G_z\rangle,\quad |2\tfrac{1}{2}\tfrac{3}{2}2G_z\rangle;$$

$G=2,\ F=\frac{5}{2}$:

$$|2\tfrac{3}{2}\tfrac{5}{2}2G_z\rangle,\quad |2\tfrac{1}{2}\tfrac{5}{2}2G_z\rangle,\quad |4\tfrac{3}{2}\tfrac{5}{2}2G_z\rangle;$$

etc. For the radial functions a system of differential eigenvalue equations results

$$\sum_{L'J'F'G'G_z'}\langle LJFGG_z|H_x|L'J'F'G'G_z'\rangle f_{L'J'F'G'G_z'}(r) = Ef_{LJFGG_z}(r). \tag{9}$$

The matrix elements of H_x are radial operators and can be established by standard methods of angular momentum calculus.[9,17] Since H_0 couples only radial functions of identical F and G the corresponding matrix separates into blocks of size 3×3 at most. Of these blocks, only those are retained which operate on at least one S-type state, i.e., we truncate series (6) after $G=2, F=\frac{3}{2}$. In the sequence of basis functions as given in (8) the matrix for H_0 is

for G arbitrary, $F=\frac{1}{2}$:

$$\begin{bmatrix} -\left(\frac{d^2}{dr^2}+\frac{2}{r}\frac{d}{dr}\right)-\frac{2}{r}-q\,\frac{\delta(r)}{4\pi r^2} & \mu\sqrt{2}\left(\frac{d^2}{dr^2}+\frac{5}{r}\frac{d}{dr}+\frac{3}{r^2}\right) \\ \mu\sqrt{2}\left(\frac{d^2}{dr^2}-\frac{1}{r}\frac{d}{dr}\right) & \lambda-(1+\mu)\left(\frac{d^2}{dr^2}+\frac{2}{r}\frac{d}{dr}-\frac{6}{r^2}\right)-\frac{2}{r} \end{bmatrix}, \tag{10}$$

for G arbitrary, $F=\frac{3}{2}$:

$$\begin{bmatrix} \lambda-\left(\frac{d^2}{dr^2}+\frac{2}{r}\frac{d}{dr}\right)-\frac{2}{r}-q\,\frac{\delta(r)}{4\pi r^2} & \mu\left(\frac{d^2}{dr^2}+\frac{5}{r}\frac{d}{dr}+\frac{3}{r^2}\right) & -\mu\left(\frac{d^2}{dr^2}+\frac{5}{r}\frac{d}{dr}+\frac{3}{r^2}\right) \\ \mu\left(\frac{d^2}{dr^2}-\frac{1}{r}\frac{d}{dr}\right) & \lambda-\left(\frac{d^2}{dr^2}+\frac{2}{r}\frac{d}{dr}-\frac{6}{r^2}\right)-\frac{2}{r} & \mu\left(\frac{d^2}{dr^2}+\frac{2}{r}\frac{d}{dr}-\frac{6}{r^2}\right) \\ -\mu\left(\frac{d^2}{dr^2}-\frac{1}{r}\frac{d}{dr}\right) & \mu\left(\frac{d^2}{dr^2}+\frac{2}{r}\frac{d}{dr}-\frac{6}{r^2}\right) & -\left(\frac{d^2}{dr^2}+\frac{2}{r}\frac{d}{dr}-\frac{6}{r^2}\right)-\frac{2}{r} \end{bmatrix}. \tag{11}$$

H_{ex} acts only on $S(L=0)$-like states of $G=1$. The nonvanishing matrix elements are (independent of G_z)

$$\langle 0\tfrac{1}{2}\tfrac{1}{2}\,1G_z|H_{ex}|0\tfrac{1}{2}\tfrac{1}{2}\,1G_z\rangle=\tfrac{2}{3}c\,\frac{\delta(r)}{4\pi r^2},$$

$$\langle 0\tfrac{1}{2}\tfrac{1}{2}\,1G_z|H_{ex}|0\tfrac{3}{2}\tfrac{3}{2}1G_z\rangle=-\frac{2\sqrt{2}}{3}c\frac{\delta(r)}{4\pi r^2}, \tag{12}$$

$$\langle 0\tfrac{3}{2}\tfrac{3}{2}1G_z|H_{ex}|0\tfrac{3}{2}\tfrac{3}{2}1G_z\rangle=\tfrac{4}{3}\,c\,\frac{\delta(r)}{4\pi r^2}.$$

2. Strain Hamiltonian and symmetries

The eigenstates for $G=0,1,2$ transform according to the irreducible representations D_0^+, D_1^+, and D_2^+ of O(3). Upon reduction to cubic symmetry and multiplication by Γ_2^+, they describe excitons of the following symmetries:

$$D_0^+\times\Gamma_2^+=\Gamma_1^+\times\Gamma_2^+=\Gamma_2^+,$$

$$D_1^+\times\Gamma_2^+=\Gamma_4^+\times\Gamma_2^+=\Gamma_5^+, \tag{13}$$

$$D_2^+\times\Gamma_2^+=(\Gamma_3^++\Gamma_5^+)\times\Gamma_2^+=\Gamma_3^++\Gamma_4^+.$$

The $G=0$ state represents the optically inactive paraexciton of symmetry Γ_2^+. The $G=2$ state describes the Γ_3^+ and Γ_4^+ paraexcitons, which are quadrupole and magnetic dipole active. The $G=1$ state is the quadrupole-active orthoexciton of Γ_5^+ symmetry which has been observed by the resonance-enhanced Raman scattering method. The strain Hamiltonian for $T\|[100]$ and [111] is of cylindrical symmetry $D_{\infty h}$, whereas the actual point symmetry of the strained crystal is D_{4h} and C_{3v}, respectively. In Table I the reduction of the O(3) irreducible representations to those of $D_{\infty h}$, i.e., the splitting of the $G=0, 1, 2$, excitons, together with the corresponding basis functions, is presented. The actual exciton symmetries are obtained by reducing the $D_{\infty h}$ irreducible representations to those of D_{4h} and C_{3v} and multiplying the resulting representations by Γ_3^+ and Γ_2, respectively. Γ_3^+ and Γ_2 are subduced from Γ_2^+ when the crystal point symmetry is lowered from O_h to D_{4h} and C_{3v}. According to Table I, the $G=1$ (Γ_5^+) exciton splits into a doubly degenerate level of (Π_g, Γ_5^+, Γ_3) and a nondegenerate level of (Σ_g^-, Γ_4^+, Γ_1) symmetry (with respect to $D_{\infty h}, D_{4h}, C_{3v}$). Stress $T\|[110]$ causes a deformation of the cubic cell of Cu_2O to a rhombohedron of symmetry D_{2h} which is also the symmetry of the strain Hamiltonian. The lowering of the symmetry to C_{2v} is caused by an asymmetric displacement of the atoms within the cell which cannot be accounted for by the continuum approximation of effective mass theory. Since the strain Hamiltonian has less than cylindrical symmetry, linear combinations of the kets $|G, G_z\rangle$ have to be taken as basis functions. These are presented in Table II, together with the irreducible representations according to which they transform under the operations of D_{2h} and of C_{2v}. Only states belonging to the same irreducible representation are coupled by the strain Hamiltonian. A close inspection of Tables I and II shows that for the computation of the exciton energies the system of coupled differential equations is at most of size 8×8. In a very concise notation the shear strain part of the radial Hamiltonian can be written as

$$\begin{pmatrix} 0 & x_1 R_1 & -\sqrt{3}\,x_2 R_1 \\ x_1 R_1^+ & -\tfrac{1}{2}x_1 R_2 & -\tfrac{1}{2}\sqrt{3}\,x_2 R_2 \\ -\sqrt{3}\,x_2 R_1^+ & -\tfrac{1}{2}\sqrt{3}\,x_2 R_2 & \tfrac{1}{2}x_3 R_2 \end{pmatrix}, \tag{14}$$

where R_1, R_2 are the matrices

$$R_1=\begin{pmatrix} 1/\sqrt{2} & 0 & 0 \\ 0 & \frac{1}{5} & \frac{1}{10} \end{pmatrix},$$

$$R_2=\begin{pmatrix} 1 & 0 & 0 \\ 0 & -\frac{3}{5} & -\frac{2}{5} \\ 0 & -\frac{2}{5} & 0 \end{pmatrix}.$$

The sequence of the basis functions is chosen as in Tables I and II and in (8). The strain constants x_1, x_2, x_3 for the different states are listed in Table III.

3. Perturbation calculation and exchange-strain splitting

Several authors have solved the effective-mass equations by a perturbation procedure, and many experiments have been interpreted in the past using this procedure. In order to connect with the present model, we also start out by considering the exchange and strain Hamiltonian H_{ex} and H_d as a perturbation of H_0. Within the space spanned by the states of quantum number $F=\frac{1}{2}, \frac{3}{2}$ ($G=0, 1, 2$), we obtain twelve decoupled eigen-

TABLE I. Exciton symmetries for $T\|[100]$ and [111]. In column 1 the exciton symmetries in the spherical model are listed. In column 2 the splitting into irreducible representations of $D_{\infty h}$ and the corresponding basis functions $|G, G_z\rangle$ are presented. In columns 3 and 4 the exciton symmetries for the actual crystal point groups D_{4h} and C_{3v} are given.

Irreducible representations of O(3) (O_h)	$D_{\infty h}$	D_{4h}	C_{3v}
D_0^+ ($^1\Gamma_2^+$)	Σ_g^+; $\|00\rangle$	$\Gamma_1^+\times\Gamma_3^+=\Gamma_3^+$	$\Gamma_1\times\Gamma_2=\Gamma_2$
D_1^+ ($^3\Gamma_5^+$)	Σ_g^-; $\|10\rangle$	$\Gamma_2^+\times\Gamma_3^+=\Gamma_4^+$	$\Gamma_2\times\Gamma_2=\Gamma_1$
	Π_g; $\|11\rangle$, $\|1-1\rangle$	$\Gamma_5^+\times\Gamma_3^+=\Gamma_5^+$	$\Gamma_3\times\Gamma_2=\Gamma_3$
	Σ_g^+; $\|20\rangle$	$\Gamma_1^+\times\Gamma_3^+=\Gamma_3^+$	$\Gamma_1\times\Gamma_2=\Gamma_2$
D_2^+ ($^2\Gamma_3^+ + {}^3\Gamma_4^+$)	Π_g; $\|21\rangle$, $\|2-1\rangle$	$\Gamma_5^+\times\Gamma_3^+=\Gamma_5^+$	$\Gamma_3\times\Gamma_2=\Gamma_3$
	Δ_g; $\|22\rangle$, $\|2-2\rangle$	$(\Gamma_3^+ + \Gamma_4^+)\times\Gamma_3^+ = \Gamma_1^+ + \Gamma_2^+$	$\Gamma_3\times\Gamma_2=\Gamma_3$

TABLE II. Exciton symmetries for $T\|[110]$. In column 2 basis functions and their symmetry for the rhombohedral strain Hamiltonian are listed. In column 3 the symmetry of the states for the actual crystal point group C_{2v} is given.

Irreducible representations of O(3) (O_h)	D_{2h}	C_{2v}
D_0^+ (${}^1\Gamma_2^+$)	Γ_1^+; $\|00\rangle$	$\Gamma_1\times\Gamma_2=\Gamma_2$
	Γ_2^+; $(\|11\rangle+\|1-1\rangle)/\sqrt{2}$	$\Gamma_2\times\Gamma_2=\Gamma_1$
D_1^+ (${}^3\Gamma_5^+$)	Γ_3^+; $\|10\rangle$	$\Gamma_3\times\Gamma_2=\Gamma_4$
	Γ_4^+; $(\|11\rangle-\|1-1\rangle)/\sqrt{2}$	$\Gamma_4\times\Gamma_2=\Gamma_3$
	Γ_1^+; $\|20\rangle$	$\Gamma_1\times\Gamma_2=\Gamma_2$
	Γ_1^+; $(\|22\rangle+\|2-2\rangle/\sqrt{2}$	$\Gamma_1\times\Gamma_2=\Gamma_2$
D_2^+ (${}^2\Gamma_3^+ + {}^3\Gamma_4^+$)	Γ_2^+ $(\|21\rangle-\|2-1\rangle)/\sqrt{2}$	$\Gamma_2\times\Gamma_2=\Gamma_1$
	Γ_3^+ $(\|22\rangle-\|2-2\rangle)/\sqrt{2}$	$\Gamma_3\times\Gamma_2=\Gamma_4$
	Γ_4^+ $(\|21\rangle+\|2-1\rangle)/\sqrt{2}$	$\Gamma_4\times\Gamma_2=\Gamma_3$

states of H_0:

$$
\begin{aligned}
|yGG_z\rangle &= F_0(r)\,|0\tfrac{1}{2}\tfrac{1}{2}GG_z\rangle + G_0(r)\,|2\tfrac{3}{2}\tfrac{1}{2}GG_z\rangle\,, \\
|gGG_z\rangle &= F_1(r)\,|0\tfrac{3}{2}\tfrac{3}{2}GG_z\rangle + G_1(r)\,|2\tfrac{3}{2}\tfrac{3}{2}GG_z\rangle \\
&\quad + G_2(r)\,|2\tfrac{1}{2}\tfrac{3}{2}GG_z\rangle\,.
\end{aligned} \tag{15}
$$

The states were denoted y if their $L=0$ part contained the hole states from the Γ_7^+ valence band ($J=\frac{1}{2}$), and g if from the Γ_8^+ valence band ($J=\frac{3}{2}$).

TABLE III. Coefficients for the strain Hamiltonian (14). The excitonic states are denoted by their transformation properties under the symmetry group of the strain Hamiltonian and the actual crystal point group.

$T\|[100]$:	
$(\Sigma_g^+,\ \Gamma_3^+)$:	$x_1=-2x_u,\ x_2=0,\ x_3=0.$
$(\Sigma_g^-,\ \Gamma_4^+)$:	$x_1=-2x_u,\ x_2=0,\ x_3=0.$
$(\Pi_g,\ \Gamma_5^+)$:	$x_1=x_2=x_3=x_u.$
$(\Delta_g,\ \Gamma_1^+ +\Gamma_2^+)$:	$x_1=x_2=0,\ x_3=-2x_u.$
$T\|[111]$:	
$(\Sigma_g^+,\ \Gamma_2)$:	$x_1=-2x_u',\ x_2=0,\ x_3=0.$
$(\Sigma_g^-,\ \Gamma_1)$:	$x_1=-2x_u',\ x_2=0,\ x_3=0.$
$(\Pi_g,\ \Gamma_3)$:	$x_1=x_2=x_3=x_u'.$
$(\Delta_g,\ \Gamma_3)$:	$x_1=x_2=0,\ x_3=-2x_u'.$
$T\|[110]$:	
$(\Gamma_1^+,\ \Gamma_2)$:	$x_1=x_3=-\frac{1}{2}(x_u+3x_u'),\ x_2=\frac{1}{2}(x_u-x_u').$
$(\Gamma_2^+,\ \Gamma_1)$:	$x_1=x_3=x_u,\ x_2=x_u'.$
$(\Gamma_3^+,\ \Gamma_4)$:	$x_1=x_3=-\frac{1}{2}(x_u+3x_u'),\ x_2=-\frac{1}{2}(x_u-x_u').$
$(\Gamma_4^+,\ \Gamma_3)$:	$x_1=x_3=-\frac{1}{2}(x_u-3x_u'),\ x_2=+\frac{1}{2}(x_u+x_u').$

Their unperturbed energies are denoted $E(y)$ and $E(g)$, respectively. For illustration we treat for tetragonal strain ($T\|[100]$) only the lowest orthoexcitons transforming according to (Σ_g^-, Γ_4^+) and (Π_g, Γ_5^+).

(i) For symmetry (Σ_g^-, Γ_4^+) the states $|y10\rangle$ and $|g10\rangle$ interact. The secular matrix is

$$
\begin{bmatrix}
E(y)+hT-\frac{2}{3}J_y & \frac{2}{3}\sqrt{2}\,J-e\sqrt{2}\,T \\
\frac{2}{3}\sqrt{2}\,J-e\sqrt{2}\,T & E(g)+hT+dT-\frac{4}{3}J_g
\end{bmatrix}, \tag{16}
$$

where

$$
\begin{aligned}
J_y &= -cF_0^2(0)/4\pi\,, \\
J &= -cF_0(0)F_1(0)/4\pi\,, \\
J_g &= -cF_1^2(0)/4\pi\,,
\end{aligned}
$$

and

$$
\begin{aligned}
eT &= x_u\int_0^\infty dr\,r^2\Big(F_0(r)F_1(r)+\frac{\sqrt{2}}{5}G_0(r)G_1(r) \\
&\qquad +\frac{\sqrt{2}}{10}G_0(r)G_2(r)\Big)\,, \\
hT &= x_h \\
dT &= x_u\int_0^\infty dr\,r^2[F_1^2(r)-\tfrac{3}{5}G_1^2(r) \\
&\qquad -\tfrac{4}{5}G_1(r)G_2(r)]\,.
\end{aligned}
$$

(ii) For symmetry (Π_g, Γ_5^+) the states $|y11\rangle$, $|g11\rangle$, and $|g21\rangle$ interact. The matrix to be diagonalized is

$$
\begin{bmatrix}
E(y)+hT-\frac{2}{3}J_y & eT/\sqrt{2}+\frac{2}{3}\sqrt{2}\,J & -\sqrt{3/2}\,eT \\
eT/\sqrt{2}+\frac{2}{3}\sqrt{2}\,J & E(g)+hT-\frac{1}{2}dT-\frac{4}{3}J_g & -\frac{1}{2}\sqrt{3}\,dT \\
-\sqrt{3/2}\,eT & -\frac{1}{2}\sqrt{3}\,dT & E(g)+hT+\frac{1}{2}dT
\end{bmatrix}. \tag{17}
$$

The secular matrices become identical to those found by Waters *et al.*[7] if $e\cong d$, i.e., if the admixture of D-like terms (G_0, G_1, G_2) is small and $F_0 \cong F_1$, and if we identify

$$E(y) = E_c^y - \tfrac{1}{2}J_y,$$

$$E(g) = E_c^G + \Delta - \tfrac{1}{2}J_g.$$

The energy eigenvalues resulting from this second-order perturbation calculation have been formulated in Ref. 7. Here we only cite the energy difference between doublets (Π_g symmetry) and singlets (Σ_g^- symmetry) for the yellow and green strain-split orthoexcitons:

$$E(y\Pi_g) - E(y\Sigma_g^-) = -4JeT/\Delta' < 0\,, \qquad (18)$$

where $\Delta' = E(g) - E(y)$,

$$E(g\Pi_g) - E(g\Sigma_g^-)$$
$$= -\tfrac{3}{2}dT + 4JeT/\Delta' - \tfrac{3}{2}e^2T^2/\Delta' + \tfrac{9}{16}d^2T^2 > 0. \qquad (19)$$

Generally we can assume $J < 0$, $e > 0$, $d > 0$, $T < 0$ (if the stress is compressive), and, for Cu_2O, $\Delta' = E(g) - E(y) > 0$. The yellow doublet and singlet are split by a second-order effect produced simultaneously by the exchange and strain interactions. This exchange-strain splitting, which has been investigated by Elliott,[18] Kiselev and Zhilich,[19] and others, places the doublet below the singlet. The splitting for the green exciton is predominantly caused by a first-order effect, namely by the strain splitting of the Γ_8^+ valence band. We expect this splitting to be much stronger than that of the yellow exciton, and the sequence of the split levels to be reversed (doublet above singlet).

III. NUMERICAL SOLUTION AND COMPARISON WITH EXPERIMENT

A. Numerical calculations

Using the quadrupole-dipole Raman scattering technique, involving odd parity phonons, Waters *et al.* measured the first four dipole-forbidden states of Γ_5^+ symmetry of the yellow series under uniaxial stress T up to 2.5 kbars (Ref. 7) parallel to [100]. They found that the triply degenerate 1S state splits into a singlet and doublet with the singlet energy increasing and the doublet energy decreasing with stress, as first observed by Gross and Kaplyanski.[20] For the higher quadrupole states, however, the sense of the splitting was reversed from that of the 1S. The magnitude of the "3S" splitting exceeded that of the 1S as noted by Agekyan and Stepanov.[6] Experiments for stress applied along the [110] direction were also reported by Waters.[21] Here the degeneracy of the Γ_5^+ orthoexciton is completely lifted. Again, as compared to the 1S yellow exciton, the sense of the splitting for the higher excitons is reversed. An attempt was made to interpret the data by exact diagonalization of the perturbation matrices (16) and (17). Only moderate agreement could be achieved with the experimental results; the level reversal could not be explained. The analysis of the quadratic strain coefficients suggested that the "3S" yellow exciton may actually belong to the green exciton series or that interactions between yellow and green excitons with different principal quantum numbers may be significant although not included in the theory. Therefore it appeared necessary to solve the radial differential eigenvalue problem (9), as has been done by Fröhlich *et al.*[8] for the case of zero stress.

We expanded the S-like radial functions ($L=0$) into exponentials $\exp(-\alpha_i r)$, the D-like radial functions into functions of the form $r\exp(-\beta_i r)$ for a fixed set of parameters α_i, β_i. The resulting general secular problem was solved numerically. The band parameters and deformation potentials were chosen to yield an optimum fit for the experimental excitonic spectra both under tetragonal and rhombohedral stress, where the zero-stress position of the 1S green exciton was assumed at 17 247 cm^{-1}. In Table IV we have listed the exciton energies for zero stress in comparison with experimental values. A notation similar to that of Fröhlich *et al.*[8] is used; the previous notations (as presented, for instance, in Ref. 5) are indicated. Apart from the 1SG paraexciton the agreement is excellent up to the 3S excitonic states and is within 1 meV also for the higher states.

In Figs. 1 and 2 the stress data are presented. The theory agrees well with the stress dependence of the level positions, the level reversal of higher excitonic states with respect to 1SY, the large strain splitting of 2SY, and the small strain splittings of 3$(SD)Y$ and 3$(DS)Y$. The splitting of the 1SG exciton, which has not been seen in the resonance Raman scattering experiments, is surprisingly small, in agreement with the observations of Agekyan and Stepanov.[6] There are other levels transforming according to Γ_5^+ for tetragonal stress and according to Γ_1, Γ_3, and Γ_4 for rhombohedral stress, which arise from the strain-split $(^2\Gamma_3^+ + {}^3\Gamma_4^+)$ ($G=2$) exciton. Of these only the Γ_3 branch of the 1SG paraexciton (at 17 183 cm^{-1}) has been drawn in Fig. 2, which displays an anticrossing effect with the Γ_3 branch of the 1SG orthoexciton (at 17 247 cm^{-1}) as the rhombohedral stress increases. The Γ_1 component of all but the 1SY orthoexciton could not be observed by Waters[21] for $T \| [110]$ due to technical difficulties.

B. Discussion

The sequence of the strain split components of the 1SY orthoexciton can be explained by the ex-

TABLE IV. Comparison of calculated energies with experimental values for zero stress. Also indicated is the old notation as presented in Ref. 5.

Present theory	Experiment	Symmetry	New notation	Old Notation
16 299	16 299	${}^1\Gamma_2^+$	1*SY* para	
16 399	16 399	${}^3\Gamma_5^+$	1*SY* ortho	1*S*
17 183	17 160	${}^3\Gamma_4^+ + {}^2\Gamma_3^+$	1*SG* para	
17 245	17 247	${}^3\Gamma_5^+$	1*SG* ortho	
17 251		${}^1\Gamma_2^+$	2*SY* para	
17 377	17 381	${}^3\Gamma_5^+$	2*SY* ortho	3*S*
17 419		${}^1\Gamma_2^+$	3*SY* para	
17 427	17 428	${}^3\Gamma_5^+$	3(*SD*)*Y* ortho	$3D_1$
17 441	17 441	${}^3\Gamma_4^+ + {}^2\Gamma_3^+$	3*DY* para	$3D_2$
17 455	17 451	${}^3\Gamma_5^+$	3(*DS*)*Y* ortho	4*S*
17 475		${}^1\Gamma_2^+$	4*SY* para	
17 478	17 470	${}^3\Gamma_5^+$	4(*SD*)*Y* ortho	$4D_1$
17 484	17 476	${}^3\Gamma_4^+ + {}^2\Gamma_3^+$	4*DY* para	$4D_2$
17 492	17 481	${}^3\Gamma_5^+$	4(*DS*)*Y* ortho	5*S*

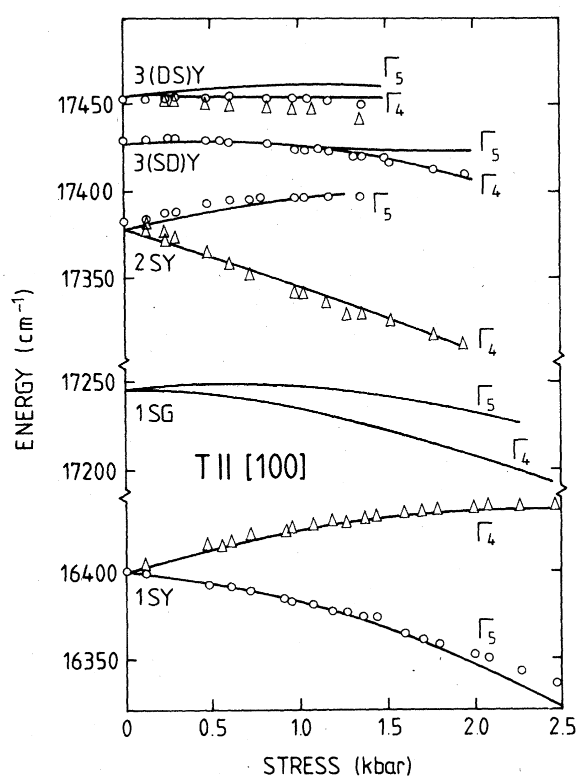

FIG. 1. Dependence of the lowest quadrupole active orthoexcitons on stress $T \parallel [100]$. Triangles denote the experimental data of Waters *et al.* for Γ_4 excitons, circles for Γ_5 excitons. No separation of the two representations was possible for the state at 17 430 cm^{-1}. Full lines are theoretical results.

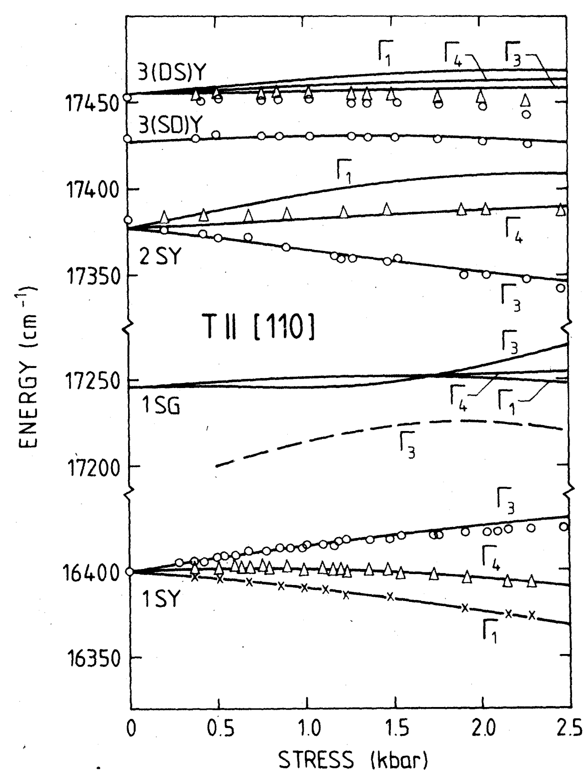

FIG. 2. Energies of orthoexcitions for rhombohedral stress $T \parallel [1\bar{1}0]$. Triangles denote the experimental data for Γ_4, circles for Γ_3, and crosses for Γ_1. Full lines are results of the present theory. The broken line is the Γ_3 branch of the strain split 1*SG* paraexciton.

change-strain splitting which is a result of perturbation theory (Sec. II B 3.). To understand the level reversal for the $2SY$ orthoexciton attention has to be paid to the strong exchange interaction between the $1SG$ and $2SY$ orthoexcitons which, according to Fröhlich *et al.*[8], diminishes the intensity of $1SG$ by shifting oscillator strength to $2SY$. Without this exchange interaction, the eigenvalue problem of the orthoexcitons reduces to that of the paraexcitons. At zero stress the $1SG$ paraexciton (at 17 183 cm^{-1}) is a mixture of 80% green S-type ($L=0$, $J=\frac{3}{2}$, $F=\frac{3}{2}$), 2% green D-type ($L=2$, $J=\frac{3}{2}$, $F=\frac{3}{2}$), and 18% yellow D-type ($L=2$, $J=\frac{1}{2}$, $F=\frac{3}{2}$) states. The $2SY$ paraexciton consists of 98% yellow S-type ($L=0$, $J=\frac{1}{2}$, $F=\frac{1}{2}$) and 2% green D-type ($L=2$, $J=\frac{3}{2}$, $F=\frac{1}{2}$) states. If the analytic exchange interaction is switched on, the following numbers result.

L	J	F	$1SG$ orthoexciton	$2SY$ orthoexciton
0	$\frac{1}{2}$	$\frac{1}{2}$	87%	34%
2	$\frac{3}{2}$	$\frac{1}{2}$	1%	0%
0	$\frac{3}{2}$	$\frac{3}{2}$	9%	33%
2	$\frac{3}{2}$	$\frac{3}{2}$	0%	0%
2	$\frac{1}{2}$	$\frac{3}{2}$	3%	33%

Hence the $1SG$ exciton has become almost completely yellow ($J=\frac{1}{2}$), whereas the $2SY$ orthoexciton is a mixture of yellow S type ($J=\frac{1}{2}$), green S type ($J=\frac{3}{2}$), and yellow D type in equal parts. The strain splitting of the $2SY$ exciton will therefore be dominated by the first-order deformation potential interaction, which causes the Γ_8^+ valence band to split and which yields the doublet above the singlet. Of course, this kind of splitting is also caused by a simultaneous action of the exchange and strain potentials, but due to the closeness of the levels and the high amplitude of the wavefunctions at $r=0$ the exchange interaction is a very strong process, not accessible by perturbation theory, upon which the strain interaction is imposed as a weak effect. The smallness of the strain splitting of the $1SG$ exciton is due to the competition between exchange-strain splitting and band deformation splitting, effects which differ in sign. The $3(SD)Y$ orthoexciton comprises a rather pure yellow S-D mixture with negligible exchange-strain splitting. The $3(DS)Y$ orthoexciton displays band deformation splitting owing to a 10% green S-type admixture.

The following parameters have been used in exciton Hamiltonian (3):

$$E_g=2.175 \text{ eV}, \quad R=0.107 \text{ eV}, \quad \lambda=1.19,$$
$$\mu=0.4, \quad q=0.15, \quad c=2.11,$$
$$x_h/T=-0.006 \text{ kbar}^{-1},$$
$$x_u/T=0.074 \text{ kbar}^{-1},$$
$$x_u'/T=-0.024 \text{ kbar}^{-1}.$$

Given the dielectric constant, the conduction-band mass and the cubic elastic compliance constants from the literature, the band parameters and deformation potentials of Table V were deduced from these data. The values for gap energy and spin-orbit splitting are very close to those measured.[4] From γ_1^h and μ_h there follows for the masses of the Γ_7^+ valence band and the Γ_8^+ light holes

$$m_{\Gamma_7^+} \cong m/\gamma_1^h = 0.66m,$$
$$m_{\Gamma_8^+}^{lh} \cong m/[\gamma_1^h(1+\mu)] = 0.40m.$$

$m_{\Gamma_7^+}$ agrees well with the cyclotron resonance data of Hodby *et al.*[23] ($m_{\Gamma_7^+}=0.69m$), $m_{\Gamma_8^+}^{lh}$ is about 30% smaller ($m_{\Gamma_8^+}^{lh}=0.58m$). The analytic exchange constant is an order of magnitude larger than that, for instance, in GaAs[15]. The shear deformation potential D_u' differs in sign from D_u. Otherwise for rhombohedral stress the Γ_3 and Γ_4 branches of each strain-split level would exactly exchange their position, as can be seen from the strain Hamiltonian [(14) and Table III]. A curious consequence of this sign difference, which also exists for CuCl[25], is that for stress parallel to the [111] direction the sequence of doubly (Γ_3) and nondegenerate levels (Γ_1) is reversed as com-

TABLE V. Crystal parameters of Cu_2O used or derived in fitting the experimental exciton data.

$\epsilon_0=7.11$ (Ref. 22)
$\epsilon_\infty=6.46$ (Ref. 22)
$E_g=2.175$ eV
$\Lambda=0.128$ eV
$R=0.107$ eV
$m_e=0.99m$ (Ref. 23)
$\gamma_1^h=1.52$
$\mu_h=0.66$
$a_a=\frac{2m}{\hbar^2}\frac{C}{4\pi e^2}=0.276$ eV^{-1}
$Q=qR=0.016$ eV
$S_{11}=4.169\times10^{-3}$ $kbar^{-1}$ (Ref. 24)
$S_{12}=-1.936\times10^{-3}$ $kbar^{-1}$ (Ref. 24)
$S_{44}=8.264\times10^{-3}$ $kbar^{-1}$ (Ref. 24)
$C_1-D_1=-2.1$ eV
$D_u=1.95$ eV
$D_u'=-0.95$ eV

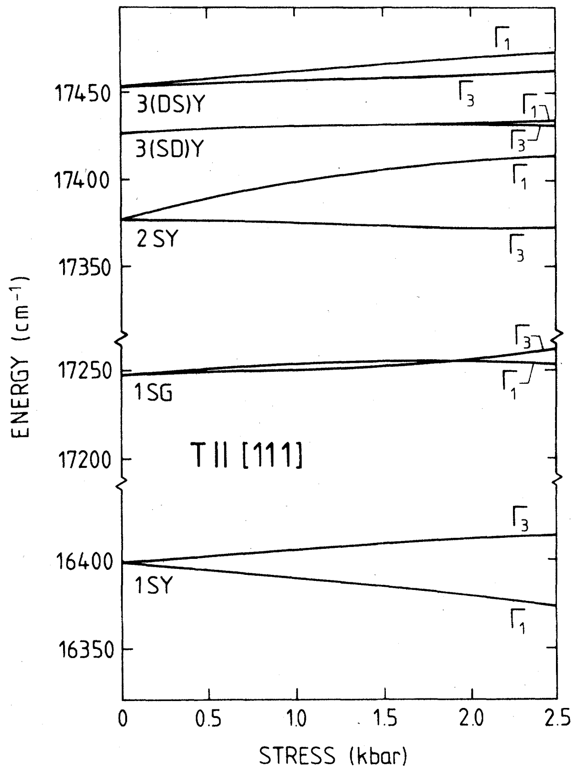

FIG. 3. Theoretical results for the orthoexciton levels under stress $T \parallel [111]$. The order of doublets (Γ_3) and singlets (Γ_1) is reversed with respect to the case $T \parallel [100]$.

pared to the case $T \parallel [100]$. The strain dependence for $T \parallel [111]$, which has not yet been measured, is presented in Fig. 3.

In our calculations the interaction of the excitons with longitudinal optical phonons (Fröhlich interaction) has been neglected, since the coupling constant is small ($\alpha \sim 0.3$). The band parameters should be considered as polaron parameters.

IV. SUMMARY

We have diagonalized the effective-mass Hamiltonian for excitons in uniaxially stressed Cu_2O in a nonperturbative approach, following the calculations of Fröhlich *et al.*[8] for the zero-stress case. The results explain the data of Waters *et al.*[7,21] The position of the 1*S* green orthoexciton between the 1*S* and 2*S* yellow orthoexciton lines is confirmed. The splitting of the 1*S* yellow exciton is understood by the mechanism of exchange-strain interaction. The splitting pattern of the 2*S* yellow orthoexciton is actually that of a green exciton, i.e., dominated by the deformation potential splitting of the Γ_8^+ valence band and reversed with respect to that of the 1*S* yellow exciton. This green character is transferred to the 2*S* yellow exciton by a strong exchange interaction with the 1*S* green exciton. The exchange-strain interaction and deformation potential interaction compete and almost cancel each other for the 1*S* green exciton, leading to a marginal splitting, which originally motivated Agekyan and Stepanov[6] to dispute the traditional level assignment scheme for even parity excitons in Cu_2O.

ACKNOWLEDGMENTS

The help of Dr. R.G. Waters and Mr. J. Wicksted in preparing the data is greatly appreciated. This work was supported by Deutsch Forschungsgemeinschaft, by the National Science Foundation under Grants Nos. DMR77-23788 and DMR78-12399, and by PSC-BHE (CUNY) Grants Nos. 13404 and 11697.

*Present address: Institut für Theoretische Physik der Universität, D-8400 Regensburg, West-Germany.

[1]J. L. Deiss, A. Daunois, and S. Nikitine, Phys. Status Solidi B 47, 185 (1971).
[2]J. C. Merle, C. Wecker, A. Daunois, J. L. Deiss, and S. Nikitine, Surf. Sci. 37, 347 (1973).
[3]V. T. Agekyan, B. S. Monozon, and I. P. Shiryapov, Phys. Status Solidi B 66, 359 (1974).
[4]T. Itoh and S. Narita, J. Phys. Soc. Jpn. 39, 132 (1975).
[5]M. A. Washington, A. Z. Genack, H. Z. Cummins, R. H. Bruce, A. Compaan, and R. A. Forman, Phys. Rev. B 15, 2145 (1977).
[6]V. T. Agekyan and Yu. A. Stepanov, Fiz. Tverd. Tela. (Leningrad) 17, 1592 (1975) [Sov. Phys.—Solid State 17, 1041 (1975)].
[7]R. G. Waters, F. H. Pollak, R. H. Bruce, and H. Z. Cummins, Phys. Rev. B 21, 1665 (1980).
[8]D. Fröhlich, R. Kenklies, Ch. Uihlein, and C. Schwab, Phys. Rev. Lett. 43, 1260 (1979).
[9]A. Baldereschi and N. O. Lipari, Phys. Rev. B 8, 2697 (1973).
[10]N. O. Lipari and A. Baldereschi, Solid State Commun. 25, 665 (1978).
[11]K. Suzuki and J. C. Hensel, Phys. Rev. B 9, 4184 (1974).
[12]For the notation see G. F. Koster, J. O. Dimmock, R. G. Wheeler, and H. Statz, *Properties of the Thirty-Two Point Groups* (MIT, Cambridge, Mass., 1963).
[13]See also the discussion by H.-R. Trebin, U. Rössler, and R. Ranvaud, Phys. Rev. B 20, 686 (1979).
[14]H.-R. Trebin, Phys. Status Solidi B 81, 527 (1977).
[15]U. Rössler and H.-R. Trebin, Phys. Rev. B (in press).
[16]M. M. Denisov and V. P. Makarov, Phys. Status Solidi B 56, 9 (1973).
[17]M. Rotenberg, R. Bivins, N. Metropolis, and J. K. Wooten, *The 3-j and 6-j Symbols* (Technology Press,

Cambridge, Mass., 1951).
[18]R. J. Elliott, Phys. Rev. 124, 340 (1961).
[19]V. A. Kiselev and A. G. Zhilich, Fiz. Tverd. Tela. (Leningrad) 13, 2398 (1971) [Sov. Phys.—Solid State 13, 2008 (1972)].
[20]E. F. Gross and A. A. Kaplyanski, Fiz. Tverd. Tela. (Leningrad) 2, 2968 (1960) [Sov. Phys.—Solid State 2, 2637 (1961)].
[21]R. G. Waters, Ph.D. Thesis, City College of CUNY, New York, 1979, unpublished.
[22]M. O'Keefe, J. Chem. Phys. 39, 1789 (1963).
[23]J. W. Hodby, T. E. Jenkins, C. Schwab, H. Tamura, and D. Trivich, J. Phys. C 9, 1429 (1976).
[24]M. H. Manghani, W. S. Brower, and H. S. Parker, Phys. Status Solidi A 25, 69 (1974).
[25]T. Koda, T. Murahashi, T. Mitani, S. Sakoda, and Y. Onodera, Phys. Rev. B 5, 705 (1972).